


Topology optimization algorithm for heterogeneous anisotropic materials and structures

A.D. Novokshenov ,  D.V. Vershinin, I.I. Abdulin

Peter the Great St. Petersburg Polytechnic University, St. Petersburg, Russia

 novoksh_ad@spbstu.ru

ABSTRACT

A two-phase topology optimization method is proposed, determines not only the ratio of the phases of high and low stiffness at each point of the body, but also the angle of rotation of the axes of anisotropy. The proposed method makes it possible to significantly improve the functionality of the products being developed. The topology optimization of the two-phase material is implemented using the method of moving asymptotes, and the angle of rotation of the anisotropy axes is aligned along the main axes of the stress tensor. As an example, a rectangular elastic plate is considered, with joint constraints in the two lower corners and the force in the middle of the upper face. The problem of simultaneous optimization of phases and axes of anisotropy is solved for this plate. The obtained results are analyzed, after which the correctness of the developed algorithm is concluded.

KEYWORDS

topology optimization • method of moving asymptotes • solid isotropic material with penalization orthotropic materials • multi-material

Acknowledgements. This work has been supported by the Russian Science Foundation grant No. 22-71-00108. <https://rscf.ru/project/22-71-00108/>

Citation: Novokshenov AD, Vershinin DV, Abdulin II. Topology optimization algorithm for heterogeneous anisotropic materials and structures. *Materials Physics and Mechanics*. 2024;52(3): 22–32. http://dx.doi.org/10.18149/MPM.5232024_3

Introduction

With the fast grow of additive manufacturing technologies possibilities, it becomes possible to create complex shaped products based on topology optimization: bridges [1,2], porous structures [3], minimum-weight, symmetrically loaded wheel structures [4], and materials with required effective mechanical properties [5,6]. Until recently, most additive manufacturing technologies were limited to using a single-phase material, which limited the functionality of the products being developed. 3D printing for multiphase material is only an emerging technology, but it will certainly lead to more functional products. For example, the article [7] demonstrates the manufacture of a product obtained using two-phase topology optimization using PolyJet additive manufacturing technology, which allows printing bulk materials with a wide range of elastic modulus [8].

In the classical formulation, topology optimization is the task of finding the optimal distribution of material in a given area under certain loads and boundary conditions. The review of the articles allows us to identify 3 classes of existing topology optimization algorithms – algorithms based on optimality criteria, algorithms based on sensitivity analysis (mathematical programming methods), and so-called genetic algorithms of topology optimization [9]. The most stable method used by the authors in optimizing

structures made of anisotropic materials is the method of moving asymptotes (MMA) [10], therefore in this work it was chosen as the base optimization algorithm.

As a result of the analysis of existing sources for optimizing the phase ratio, it was observed that the most of the works on topology optimization based on density, taking into account several material phases, are based on expanding the interpolation scheme of a solid isotropic material (SIMP), which uses a power law to determine intermediate densities, taking into account various regions of a solid and voids [11,12]. To optimize the topology of two materials (without voids) [13], a single design variable is used to interpolate between two phases of the material [14]. The approach has also been used, for example, to multiphysics actuators design, [15] and functionally graded structures with optimal eigenfrequencies design [16]. A three-phase expansion of SIMP has also been proposed [14], characterized by a topology design variable that controls the material/void distribution and a second design variable that interpolates between two solid material phases. This “three-phase mixing” scheme is expandable to an arbitrary number of materials [17,18], however, it is noted that with a further increase in the number of design variables, the optimization problem, as a rule, gets stuck in a local extremum. In fact, most of the results in the papers on optimizing topology from multiple materials using this “m-phase mixing” scheme were limited to two solid phases and a void [7,19]. The multi-material topology optimization by considering the volumes of multiple materials have also been applied to other problems, including simultaneous structural and thermal analyses [20], lattice structures [21], thermal buckling criteria [22], and cable-suspended membrane structures [23].

Development of composite 3D printers [24] make actual to use topology optimization with conjunction of material anisotropy axes optimization. As a result of the analysis of existing articles on the optimization of anisotropy axes directions, several approaches have been identified to solve this problem. In particular, there are approaches that do not introduce additional design variables for the orientation of the material. Instead, it is assumed that the main direction of the material coincides with the main direction of stress tensor or deformation tensor, which is reasonable for “shear-weak” materials [25,26]. Also, there are approaches that introduce additional design variables to optimize the orientation of the material [27,28]. However, due to the difficulty of avoiding local optima [29,30], the optimization of the orientation of the material based on the stress tensor and strain tensor is used in this work.

Methods

The classic state of topology optimization problem is to determine the optimal material distribution in terms of stiffness under given boundary conditions and resource constraints. Maximizing the stiffness of a body is equivalent to minimizing the elastic energy of deformation (i.e. compliance), which has the following form:

$$c = \frac{1}{2} \int_{\Omega} ({}^4\mathbf{C} \cdot \boldsymbol{\varepsilon}) \cdot \boldsymbol{\varepsilon} d\Omega, \quad (1)$$

where ${}^4\mathbf{C}$ is an elasticity tensor; $\boldsymbol{\varepsilon}$ is a strain tensor; Ω is a material volume (design domain).

Parameterization of the optimization space is performed through finite element discretization and the application of the approach SIMP (solid isotropic material with

penalization). The properties of the material in each element depend on the magnitude of the fictitious density ρ^e , the values of which vary from 0 to 1. It is assumed that:

$${}^4\mathbf{C}^e = \rho^{ep} {}^4\mathbf{C}_0^e, \quad (2)$$

where ${}^4\mathbf{C}_0^e$ is an initial elasticity tensor in a given finite element, p is a penalization factor.

The maximum allowed volume fracture is expressed by the following inequality:

$$\int_{\Omega} \rho(\mathbf{r}) d\Omega < V, \quad (3)$$

where Ω is a design domain, $\rho(\mathbf{r})$ is a fictitious density (design variable, which vary from 0 to 1).

Thus, the problem of finding the distribution of material in the considered area in the finite element formulation will have the form (4) subject to (5) [11]:

$$\min(\mathbf{f}^T \mathbf{u}), \quad (4)$$

$$\begin{cases} \mathbf{K}\mathbf{u} = \sum_{e=1}^N \mathbf{K}^e(\rho^e) \mathbf{u}^e = \mathbf{f} \\ \mathbf{K}^e(\rho^e) = \rho^{ep} \mathbf{K}_0^e \\ \frac{V}{V_0} = \frac{\sum_{e=1}^N V^e}{V_0} = \alpha \\ 0 < \alpha < 1 \end{cases}, \quad (5)$$

where \mathbf{f}^T is a force vector, \mathbf{u} is a displacement vector, \mathbf{u}^e is a displacement vector of the element nodes, \mathbf{K} is a global stiffness matrix, $\mathbf{K}^e(\rho^e)$ is a local stiffness matrix of the element, \mathbf{K}_0^e is an initial local stiffness matrix of the element, V^e is a volume of the element, V_0 is an initial volume of the body.

To solve this problem, mathematical programming methods are further applied. In this work, the method of moving asymptotes (MMA) was used.

Topology optimization using two phases

Control of several phases in the optimization process is carried out using an extension of the SIMP method. In this work, a three-phase SIMP method (as shown in 1) was used, which is characterized by two design variables ρ_0^e and ρ_1^e [15]:

$$\mathbf{K}^e(\rho_0^e, \rho_1^e) = \rho_0^{ep_0} (\rho_1^{ep_1} \mathbf{K}_1^e + (1 - \rho_1^e)^{p_1} \mathbf{K}_2^e), \quad (6)$$

where ρ_0^e is a density of the total material in element, ρ_1^e is a ratio of the volume of phase 1 with respect to the volume of the total material in element, p_0 and p_1 are penalization factors, \mathbf{K}_1^e is an initial local stiffness matrix of the element of phase 1, \mathbf{K}_2^e is an initial local stiffness matrix of the element of phase 2.

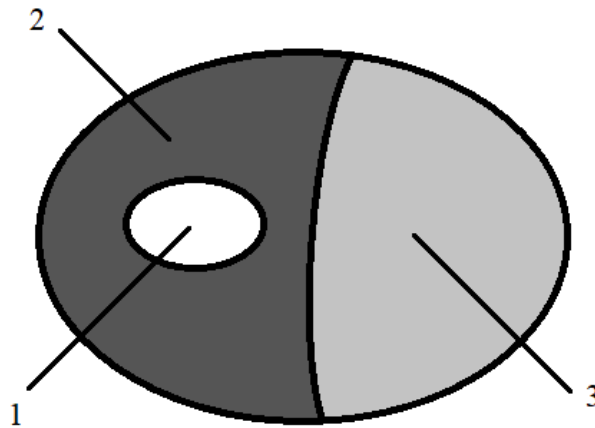


Fig. 1. 1 – void phase, 2 – phase 1, 3 – phase 2

The volume constraint for design domains of two materials can be written as (7) [31]:

$$\left\{ \begin{array}{l} \frac{V^e}{V_0} \sum_{e=1}^N (1 - \rho_0^e) = (1 - \alpha_0) \\ \frac{V^e}{V_0} \sum_{e=1}^N \rho_0^e \rho_1^e = \alpha_0 \alpha_1 \\ \frac{V^e}{V_0} \sum_{e=1}^N \rho_0^e (1 - \rho_1^e) = \alpha_0 (1 - \alpha_1) \end{array} \right. , \quad (7)$$

where α_0 is a volume fraction of the total material with respect to the volume of the design domain, α_1 is a ratio of the volume of the first phase to the volume of the total material.

The formulation of the topology optimization problem can be expressed as (8) subject to (9) [15]:

$$\begin{array}{l} \min(\mathbf{f}^T \mathbf{u}), \\ \left\{ \begin{array}{l} \mathbf{K} \mathbf{u} = \sum_{e=1}^N \mathbf{K}^e(\rho_0^e, \rho_1^e) \mathbf{u}^e = \mathbf{f} \\ \mathbf{K}^e(\rho_0^e, \rho_1^e) = \rho_0^{e p_0} (\rho_1^{e p_1} \mathbf{K}_1^e + (1 - \rho_1^e)^{p_1} \mathbf{K}_2^e) \\ \frac{V^e}{V_0} \sum_{e=1}^N (1 - \rho_0^e) = (1 - \alpha_0) \\ \frac{V^e}{V_0} \sum_{e=1}^N \rho_0^e \rho_1^e = \alpha_0 \alpha_1 \\ \frac{V^e}{V_0} \sum_{e=1}^N \rho_0^e (1 - \rho_1^e) = \alpha_0 (1 - \alpha_1) \\ 0 < \alpha_0, \alpha_1 < 1 \end{array} \right. \end{array} \quad (8) \quad (9)$$

Predicting the optimal orientation

An orthotropic material was considered. The stiffness of the structure was maximized by varying the orientation of the orthotropy axes in each finite element.

Optimization of the orthotropy axes was carried out in conjunction with topology optimization. The classical SIMP method with one design variable (10) was used, where the stiffness matrix can be expressed using a rotation tensor [32]:

$$\left\{ \begin{array}{l} \mathbf{K}^e(\varphi, \rho^e) = \rho^{e p} \mathbf{K}_0^e(\varphi) \\ \mathbf{K}_0^e(\varphi) = \mathbf{B}^T \mathbf{T}^T(\varphi) \mathbf{D} \mathbf{T}(\varphi) \mathbf{B} \det(\mathbf{J}) \end{array} \right. \quad (10)$$

where φ is a variable orientation of the orthotropy axes, $\mathbf{K}_0^e(\varphi)$ is a local stiffness matrix of the element rotated by an angle φ , \mathbf{D} is an elasticity matrix of an orthotropic material, \mathbf{B} is a matrix of the derivatives of shape functions, $\mathbf{T}(\varphi)$ is a rotation matrix, \mathbf{J} is the Jacobi matrix.

The algorithm for optimizing the distribution of the material and the angle of rotation is constructed in such a way that the design variable is only a fictitious density ρ^e . The angle φ is aligned along the main stress or strain axes before each step of the topology optimization algorithm.

The scheme of algorithm is shown in Fig. 2. The constructed algorithm consists of the following steps:

1. Changing all design variables ρ^e to satisfy the volume fraction constraint.
2. Finite element calculation of the stress-strain state of the body.
3. Calculation of the sensitivities of the strain energy by design variables (11):

$$\frac{\partial c}{\partial \rho^e}, \quad (11)$$

where $c = \mathbf{u}^T \mathbf{K} \mathbf{u}$.

4. Finding the main direction of the stress/strain tensor.

5. Construction of a convex approximation of the function, finding the minimum through the dual function (internal MMA cycle) [10].
6. The found solution is the next step of the approximation point. Updating the vector of design variables.
7. Updating direction of anisotropy axes according to main stress/strain tensor directions.
8. Checking for convergence. If there is no convergence, return to step 2.

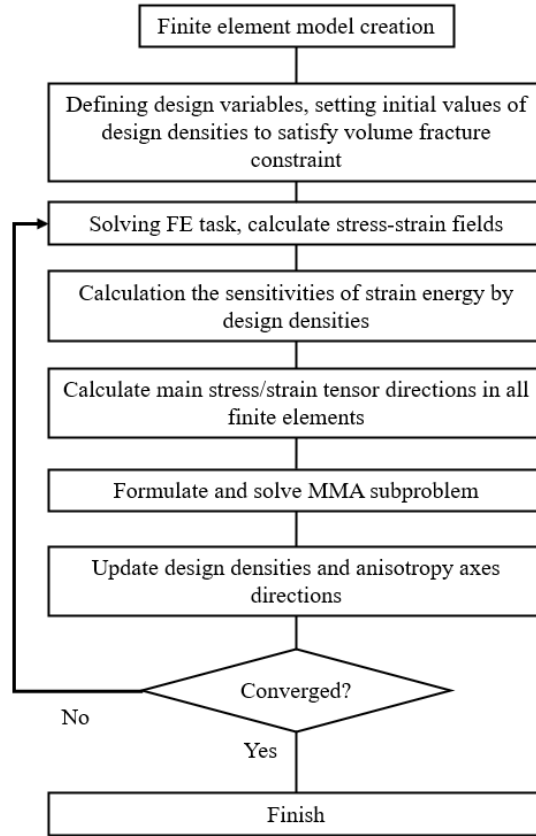


Fig. 2. Developed algorithm scheme

The formulation of the topology optimization problem can be expressed as (12) subject to (13):

$$\min(\mathbf{f}^T \mathbf{u}), \quad (12)$$

$$\begin{cases} \mathbf{K}\mathbf{u} = \sum_{e=1}^N \mathbf{K}^e(\varphi, \rho^e) \mathbf{u}^e = \mathbf{f} \\ \mathbf{K}^e(\varphi, \rho^e) = \rho^{e^p} \mathbf{K}_0^e(\varphi) \\ \frac{V}{V_0} = \frac{\sum_{e=1}^N V^e}{V_0} = \alpha \\ 0 < \alpha < 1 \end{cases} \quad (13)$$

Development of a topology optimization algorithm using two phases, taking into account the direction of the anisotropy axes

The optimization of heterogeneous orthotropic material was carried out using a combination of two approaches (14):

$$\begin{cases} \mathbf{K}^e(\varphi, \rho_0^e, \rho_1^e) = \rho_0^{e p_0} \left(\rho_1^{e p_1} \mathbf{K}_1^e(\varphi) + (1 - \rho_1^e)^{p_1} \mathbf{K}_2^e(\varphi) \right), \\ \mathbf{K}_i^e(\varphi) = \mathbf{B}^T \mathbf{T}^T(\varphi) \mathbf{D}_i \mathbf{T}(\varphi) \mathbf{B} \det(\mathbf{J}) \end{cases}, \quad (14)$$

where $\mathbf{K}_i^e(\varphi)$ is a local stiffness matrix of the element of the i -th phase, \mathbf{D}_i is an elasticity matrix of the orthotropic i -th phase.

The algorithm for optimizing the distribution of phases and the angle of rotation is the same as in the previous subsection but uses only two design variables – ρ_0^e and ρ_1^e .

The formulation of the topology optimization problem can be expressed as (15) subject to (16):

$$\begin{cases} \min(\mathbf{f}^T \mathbf{u}), \\ \mathbf{K} \mathbf{u} = \sum_{e=1}^N \mathbf{K}^e(\varphi, \rho_0^e, \rho_1^e) \mathbf{u}^e = \mathbf{f} \\ \mathbf{K}^e(\varphi, \rho_0^e, \rho_1^e) = \rho_0^{e p_0} \left(\rho_1^{e p_1} \mathbf{K}_1^e(\varphi) + (1 - \rho_1^e)^{p_1} \mathbf{K}_2^e(\varphi) \right) \\ \frac{V^e}{V_0} \sum_{e=1}^N (1 - \rho_0^e) = (1 - \alpha_0) \\ \frac{V^e}{V_0} \sum_{e=1}^N \rho_0^e \rho_1^e = \alpha_0 \alpha_1 \\ \frac{V^e}{V_0} \sum_{e=1}^N \rho_0^e (1 - \rho_1^e) = \alpha_0 (1 - \alpha_1) \\ 0 < \alpha_0, \alpha_1 < 1 \end{cases}, \quad (15)$$

Implementation of the developed topological optimization algorithms

To implement the optimization algorithm, the Python language was chosen as the most convenient and fastest from the point of view of development, as well as containing the NumPy and SciPy libraries with a large number of functions for working with matrices, including highly sparse large-dimensional matrices that arise when using the finite element method.

A proprietary 2D finite element solver has been developed, which includes not only well-known standard procedures, but also supplemented with the parameters necessary to solve the optimization problem. The finite element solver was tested on simple 2D problems of elasticity theory, the results coincided with ANSYS with high accuracy.

The MMA method did not need to be fully implemented, since an implementation of this algorithm in Python was found in open sources. However, it was necessary to adapt this program code to solve the problem of topological optimization, both in terms of algorithm settings and in terms of the connection of the algorithm with a finite element solver. In particular, a feature has been added that allows you to change the design variables in the finite element model after each completed internal MMA cycle.

To display the optimization results, a separate module was developed using the Python - matplotlib library.

Results and Discussion

Optimization of the material distribution, phases and orthotropy direction angle was tested on a two-dimensional plate with boundary conditions and loads shown in Fig. 3. Design domain with boundary conditions and load: $L=40$ mm, finite element discretization 160×40 , $F=100$ N.

The following parameters were used for each of the optimization tasks:

- number of iterations: 100;
- penalization powers: $p = p_0 = p_1 = 4$;
- volume constraints: $\frac{V}{V_0} = 0.5$, $\frac{V_1}{V_0} = \frac{V_2}{V_0} = 0.25$.

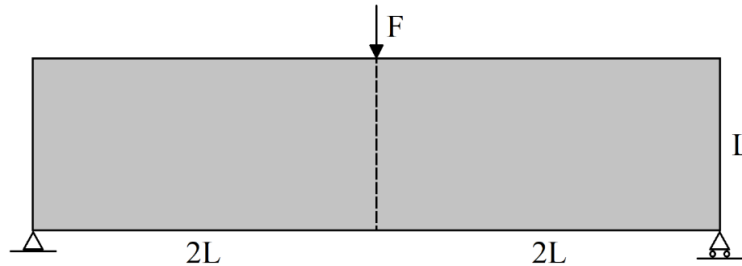


Fig. 3. Design domain with boundary conditions and loads: $L = 40$ mm, finite element discretization 160×40 , $F = 100$ N

The test materials taken from literature [15,29] are presented in Tables 1–3. The optimization results are shown in Figs.–7.

It can be seen that the phase with high stiffness is distributed along the edges as a result of optimization, which corresponds to the results given in the literature. However, the optimization results in this paper and the optimization results from the sources are slightly different, due to different optimization parameters and phase properties.

Optimization through alignment of the orthotropy axes along the main directions of the stress tensor is a more effective method compared to alignment along the main directions of the strain tensor. Firstly, the value of the objective function (strain energy) as a result of optimization for the first case turns out to be less. Secondly, alignment along the main directions of the stress tensor gives a more understandable result – the direction of the anisotropy axes in most cases agrees with the topology of the structure, that is, inside the "rod-like" structures remaining as a result of optimization, the direction of the orthotropy axes coincides with the direction of the outer boundary of these structures. In the case of alignment along the main directions of the strain tensor, the results are more unpredictable.

Finally, the simultaneous optimization of the material distribution, phases and orthotropy direction angle was tested on a plate. On Fig. 6, it can be seen that phase distribution has the same character as in the case of isotropic phases, and the anisotropy axes are consistent with the "rod-like" topology.

To demonstrate the advantages of the presented optimization, a comparative analysis of the results for the classic topology optimization algorithm and developed was performed. The results of optimization and comparison are presented in Table 4.

It can be seen from the table above that the use of two orthotropic phases and the alignment of the anisotropy axes leads to a decrease in compliance.

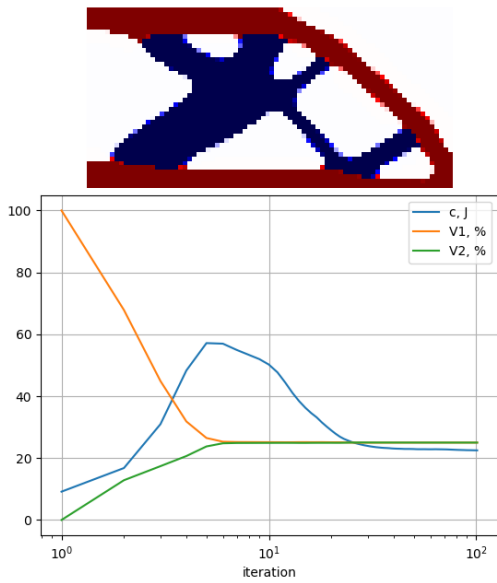


Fig. 4. Optimal distribution of isotropic phases, $c = 22.49$ J: red color – phase 1, blue color – phase 2

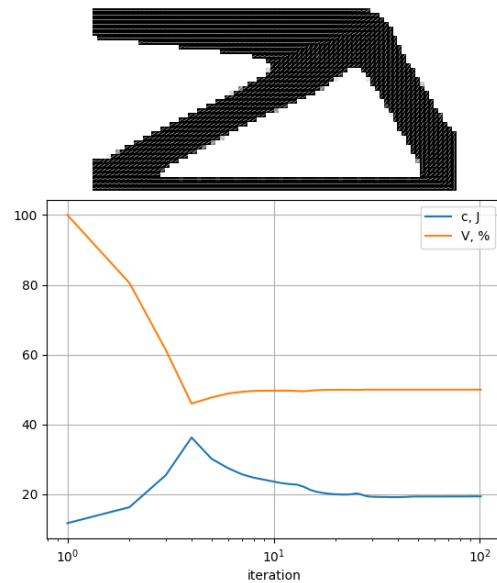


Fig. 5. Optimal distribution of orthotropic material, alignment of orthotropy axes along the main directions of the stress tensor, $c = 19.413$ J

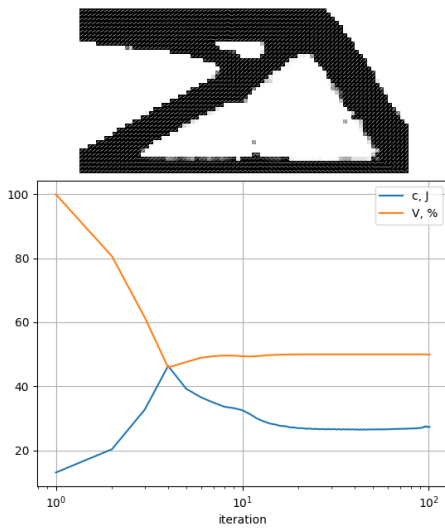


Fig. 6. Optimal distribution of orthotropic material, alignment of anisotropy axes along the main directions of the strain tensor, $c = 27.317$ J

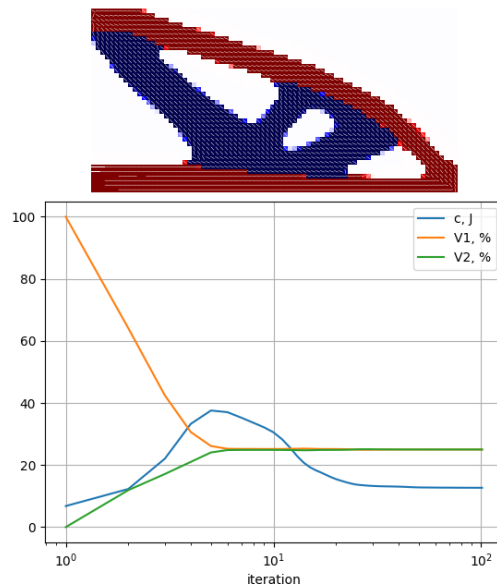


Fig. 7. Optimal distribution of orthotropic phases, alignment of anisotropy axes along the main directions of the stress tensor, $c = 12.669$ J: red color – phase 1, blue color – phase 2

Table 1. Properties of isotropic phases for the task of optimizing the phase distribution

E_1 , GPa	E_2 , GPa	ν_1	ν_2
200.00	100.00	0.31	0.31

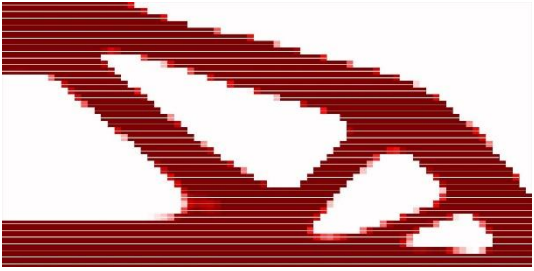
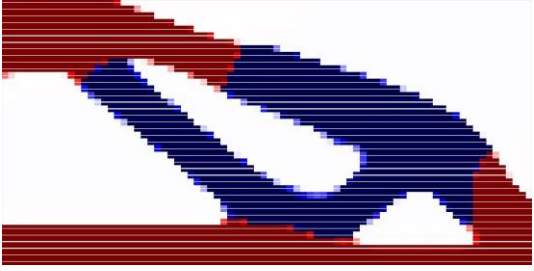
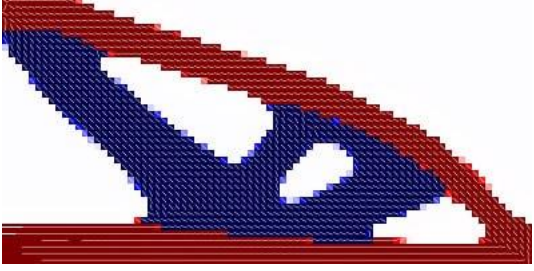
Table 2. Properties of an orthotropic material for the task of optimizing the distribution of the material and the axes of orthotropy

E_x , GPa	E_y , GPa	E_z , GPa	G_{xy} , GPa	G_{yz} , GPa	G_{xz} , GPa	ν_{xy}	ν_{yz}	ν_{xz}
54.00	18.00	18.00	9.00	9.00	9.00	0.25	0.25	0.25

Table 3. Properties of orthotropic phases for the problem of optimizing the distribution of phases and axes of orthotropy

Nº phase	E_x , GPa	E_y , GPa	E_z , GPa	G_{xy} , GPa	G_{yz} , GPa	G_{xz} , GPa	ν_{xy}	ν_{yz}	ν_{xz}
1	108.00	18.00	18.00	9.00	9.00	9.00	0.25	0.25	0.25
2	54.00	18.00	18.00	9.00	9.00	9.00	0.25	0.25	0.25

Table 4. Comparison table of optimization results for various materials (1 – topology optimization with one orthotropic material phase, 2- topology optimization with two orthotropic material phases, 3 - topology optimization with two orthotropic material phases with orthotropy axes direction variation)

Nº material	Predicting orientation	Compliance, J	Optimal distribution
1	No	72.36	
2	No	35.49	
2	No	28.23	
3	Yes	12.67	

Conclusions

In this paper, an algorithm for two-phase topology optimization was developed, taking into account the rotation of the axes of anisotropy (orthotropy).

The distribution of the two isotropic phases was compared with the results from open sources. Based on the results of the comparison, it can be said that the phase distributions are qualitatively the same.

The alignment of orthotropy direction angles along the main directions of the stress and strain tensor was compared. Alignment along the main directions of the stress tensor

is a more efficient method, which is why it was used in optimizing a heterogeneous material with two orthotropy phases and a void.

The developed algorithm was tested on the problem of topology optimization of the plate. An optimal distribution of the material with two orthotropic phases and a void was obtained, in which the phase distribution was similar to the isotropic case, and the orthotropy axes were consistent with a "rod-like" topology.

References

1. Zegard T, Paulino GH. Bridging topology optimization and additive manufacturing. *Struct. Multidiscip. Optim.* 2016;53(1): 175–192.
2. Zegard T, Paulino GH. GRAND – Ground structure based topology optimization on arbitrary 2D domains using MATLAB. *Struct. Multidiscip. Optim.* 2014;50(5): 861–882.
3. Robbins J, Owen SJ, Clark BW, Voth TE. An efficient and scalable approach for generating topology optimized cellular structures for additive manufacturing. *Addit. Manuf.* 2016;12: 296–304.
4. Dewhurst P, Srithongchai S. An investigation of minimum weight dual-material symmetrically loaded wheels and torsion arms. *J. Appl. Mech.* 2005;72(2): 196–202.
5. Borovkov AI, Maslov LB, Zhmaylo MA, Tarasenko FD, Nezhinskaya LS. Elastic properties of additively produced metamaterials based on lattice structures. *Materials Physics Mechanics.* 2023;51(7): 42–52.
6. Borovkov AI, Maslov LB, Zhmaylo MA, Tarasenko FD, Nezhinskaya LS. Finite element analysis of elastic properties of metamaterials based on triply periodic minimal surfaces. *Materials Physics Mechanics.* 2024;52(2): 63–81.
7. Gaynor AT, Meisel NA, Williams CB, Guest JK. Multiple-material topology optimization of compliant mechanisms created via polyjet three-dimensional printing. *J. Manuf. Sci. Eng.* 2014;136(6): 061015.
8. *PolyJet Materials: A range of possibilities.* Stratasys. 2016.
9. Bendsoe MP, Martin P. *Topology optimization: theory, methods and applications.* Berlin: Springer; 2003.
10. Svanberg K. The method of moving asymptotes—a new method for structural optimization. *International Journal for Numerical Methods in Engineering.* 1987;24(2): 359–373.
11. Bendsoe MP. Optimal shape design as a material distribution problem. *Struct. Optim.* 1989;1: 193–202.
12. Zhou M, Rozvany GIN. The COC algorithm, Part II: topology, geometrical and generalized shape optimization. *Comput. Methods Appl. Mech. Engrg.* 1991;89(1–3): 309–336.
13. Li M, Deng Y, Zhang H, Wong SHF, Mohamed A, Zheng Y, Gao J, Yuen TYP, Dong B, Kuang JS. Topology optimization of multi-material structures with elastoplastic strain hardening model. *Structural and Multidisciplinary Optimization.* 2021;64(3): 1141–1160.
14. Sigmund O, Torquato S. Design of materials with extreme thermal expansion using a three-phase topology optimization method. *J. Mech. Phys. Solids.* 1997;45(6): 1037–1067.
15. Sigmund O. Design of multiphysics actuators using topology optimization—Part I: Two-material structures. *Comput. Methods Appl. Mech. Engrg.* 2001;190(49–50): 6577–6604.
16. Taheri AH, Hassani B. Simultaneous isogeometrical shape and material design of functionally graded structures for optimal eigenfrequencies. *Comput. Methods Appl. Mech. Engrg.* 2014;277: 46–80.
17. Stegmann J, Lund E. Discrete material optimization of general composite shell structures. *Internat. J. Numer. Methods Engrg.* 2005;62(14): 2009–2027.
18. Sigmund O. Design of multiphysics actuators using topology optimization Part II: Two-material structures. *Comput. Methods Appl. Mech. Engrg.* 2001;190(49–50): 6605–6627.
19. Gibiansky LV, Sigmund O. Multiphase composites with extremal bulk modulus. *J. Mech. Phys. Solids.* 2000;48(3): 461–498.
20. Vantighem G, Boel V, Steeman M, Corte WD. Multi-material topology optimization involving simultaneous structural and thermal analyses. *Struct. Multidiscip. Optim.* 2019;59: 731–743.
21. Kazemi H, Vaziri A, Norato JA. Multi-material topology optimization of lattice structures using geometry projection. *Comput. Methods Appl. Mech. Engrg.* 2020;363: 112895.
22. Wu C, Fang J, Li Q. Multi-material topology optimization for thermal buckling criteria. *Comput. Methods Appl. Mech. Engrg.* 2019;346: 1136–1155.

23. Luo Y, Niu Y, Li M, Kang Z. A multi-material topology optimization approach for wrinkle-free design of cable-suspended membrane structures. *Comput. Mech.* 2017;59: 967–980.
24. Zobacheva AY, Nemov AS, Borovkov AI, Novokshenov AD, Khovaiko MV, Ermolenko NA. Design and simulation of additive manufactured structures of three-component composite material. *Materials Physics and Mechanics.* 2017;34(1): 51–58.
25. Zhou KM, Li X. Topology optimization of structures under multiple load cases using a fiber-reinforced composite material model. *Comput. Mech.* 2006;38(2): 163–170.
26. Gea H, Luo J. On the stress-based and strain-based methods for predicting optimal orientation of orthotropic materials. *Struct Multidiscip Optim.* 2004;26(3–4): 229–234.
27. Pedersen P. Examples of density, orientation, and shape-optimal 2D-design for stiffness and/or strength with orthotropic materials. *Structural and Multidisciplinary Optimization.* 2004;26(1–2): 37–49.
28. Zhou K, Li X. Topology optimization for minimum compliance under multiple loads based on continuous distribution of members. *Structural and Multidisciplinary Optimization.* 2008;37(1): 49–56.
29. Stegmann J, Lund E. Discrete material optimization of general composite shell structures. *International Journal for Numerical Methods in Engineering.* 2005;62(14): 2009–2027.
30. Ansola R, Canales J, Tarrago J, Rasmussen J. On simultaneous shape and material layout optimization of shell structures. *Structural and Multidisciplinary Optimization.* 2002;24(3): 175–184.
31. Thurier PF, Lesieutre GA, Frecker MI, Adair JH. A two-material topology optimization method for structures under steady thermo-mechanical loading. *Journal of Intelligent Material Systems and Structures.* 2019;30(11): 1717-1726.
32. Shen Y, Branscomb D. Orientation optimization in anisotropic materials using gradient descent method. *Composite Structures.* 2019;234: 111680.

About Author

Aleksei D. Novokshenov  

Candidate of Technical Sciences

Associate Professor (Peter the Great St. Petersburg Polytechnic University, St. Petersburg, Russia)

Denis V. Vershinin

Engineer (Peter the Great St. Petersburg Polytechnic University, St. Petersburg, Russia)

Ilia I. Abdulin

Engineer (Peter the Great St. Petersburg Polytechnic University, St. Petersburg, Russia)